

Angle of Arrival Estimation System for LoRa Technology based on Phase Detectors

Noori BniLam^{†,*}, Samer Nasser^{†,*}, Maarten Weyn[†]

[†]University of Antwerp - imec, IDLab - Faculty of Applied Engineering, Antwerp, Belgium

*{noori.bnalam, samer.nasser}@uantwerpen.be

Abstract—In this paper, we propose a comprehensive low-power and low-cost Angle of Arrival (AoA) estimation system. The proposed system consists of a hardware architecture and an AoA estimation algorithm. The proposed hardware captures the phase values of the received signal and transmits them to the nearest LoRaWAN gateway. In the cloud, an AoA estimation algorithm will be performed, and the AoA of the received signal will be estimated. The proposed hardware is generic, and it can estimate the AoA of any received signal that is operating at a frequency below 2.7 GHz. However, we have validated its performance with LoRa signals that are operating at the 868 MHz frequency band. The experimental validation, which has been conducted in a controlled environment, reveals that the proposed system can estimate the AoA of the received signals from various azimuth angles with median and maximum estimation errors of 4 and 14 degrees, respectively.

Index Terms—Angle of Arrival, AoA, Direction of Arrival, DoA, Internet of Things, IoT, LPWAN, LoRa, phase detector, AD8302, localization.

I. INTRODUCTION

Over the past years, there have been increasing demands for smart devices that are connected to the internet. Currently, many services depend on the connectivity of spatially distributed transceivers to the internet, and these services are only expected to grow in the future. Accordingly, the Internet of Things (IoT) industry is thriving, and low power wireless area network (LPWAN) standards (such as LoRa, Sigfox and NB-IoT) are currently deployed to provide IoT services.

Localization and tracking services are considered a key feature that distinguishes IoT standards from each other. For instance, LoRa networks provide a localization solution based on the Time Difference of Arrival (TDoA) of the received signals [1]. Sigfox and NB-IoT, on the other hand, provide localization solutions based on the Received Signal Strength (RSS) values [2], [3]. Even though the Angle of Arrival (AoA) estimation techniques have the potential to provide accurate localization solutions for IoT applications [4], commercially available AoA-based localization systems (to the best of the author's knowledge) do not yet exist for LPWAN technologies. This absence can be attributed to the complexity that is associated with implementing them. Therefore, promoting AoA-based localization systems for IoT applications can

only be achieved by reducing the system complexity, which constitutes the main objective of this paper.

AoA-based localization systems require multiple spatially distributed array antennas to provide a location estimate of the transmitting device [5], [6]. Several array antenna systems, that can provide AoA estimates for IoT networks, have been proposed lately [7]–[11]. These array antenna systems exploit Software Defined Radio (SDR) frontends with coherent RF channels (i.e. fully time synchronized and phase coherent). Coherent RF channels are difficult to implement and maintain, especially if a low-cost solution is sought. Furthermore, SDR frontends are usually considered high power consumption devices.

To avoid the requirement of coherent RF channels, several AoA solutions have been presented in the literature. Baik et al [12] have provided an AoA estimation solution based on a time modulated array (TMA) that consists of two antenna elements. Avitabile et al. [13] have provided a low cost and complexity phase detection hardware to estimate the AoA of a single received signal. Lately, solutions for AoA estimation, that are based on analog beamforming networks (BFNs), have also been presented in the literature. Notable attempts, to estimate the AoA of the received signals by deploying a Rotman lens (i.e. a BFN hardware), were conducted by Chiang et al. [14] and BniLam et al. [15].

In this paper, we propose a comprehensive low-power and low-cost AoA estimation system. The proposed system consists of a hardware architecture and an AoA estimation algorithm. The full system design is presented in Section III. The proposed hardware architecture is generic, and it can estimate the AoA of any received signal that is operating at a frequency below 2.7 GHz. However, we have validated its performance with LoRa signals that are operating at the 868 MHz frequency band. The proposed AoA algorithm (see Section IV) is simple, computationally efficient, and provides accurate AoA estimates of the received signals.

In the following, the proposed hardware architecture and the AoA estimation algorithm will be presented, followed by the experimental results and the conclusions, but first a brief introduction to the selected phase detector hardware will be presented.

II. AD8302 PHASE DETECTOR

Recently, the AD8302 phase detector module [16], [17], as shown in figure 1, has been explored to capture the phase difference of an incoming signal for AoA estimation purposes. The AD8302 is a fully integrated system for measuring gain/loss and phase in various applications. The AC-coupled input signals can range from -60 dBm to 0 dBm in a 50Ω system, from low frequencies up to 2.7 GHz. The phase (VPHS pin) and gain (VMAG pin) output voltages are simultaneously available at loadable ground referenced outputs over the standard output range of 0 V to 1.8 V, where 0 V is dedicated for π phase difference and 1.8 V is dedicated for 0 phase difference. Accordingly, as will become apparent in Section V, the AD8302 module has a phase ambiguity between the positive and the negative phase angles.

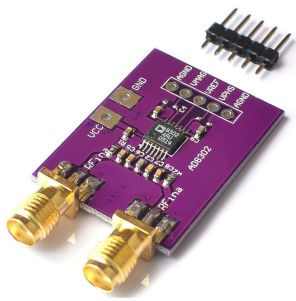


Fig. 1: AD8302 phase detector module.

Balsamo et al. [18] have utilized two AD8302 modules to provide an AoA estimation system in the 2.4 GHz frequency band. Their system constitutes two dipole antenna pairs that are orthogonal to each other. Each pair is connected to a designated AD8302 board to measure the phase and amplitude differences. Due to the aforementioned phase ambiguity, the output voltage for the positive phase difference is the same as its negative counterpart. Balsamo et al. have tackled this issue by exploiting the amplitude difference values of the two antenna pairs. They conducted an experiment to evaluate their system, where a continuously transmitting device was placed 1.5 meters away from the AoA estimation system. Their experimental results show that 68% of the estimated angles were within 10° estimation error. Balsamo et al. system is very easy to deploy and have provided a relatively good estimation accuracy. However, the system has two major drawbacks; the first is the dependency of the amplitude difference. In realistic environments, the amplitude difference will become very small when the transmitter is far away from the AoA estimation system. The second drawback is the use of a continuous signal. This assumption is absolutely invalid for a realistic communication system.

In this paper, we tackle these major drawbacks fundamentally. The phase ambiguity has been tackled by using

a triangle antenna system. The various phase difference values of the triangle antenna elements will ensure a phase uniqueness in the region between the azimuthal angles of -90° to 90° . Furthermore, an extra AD8302 module has been deployed to provide an amplitude difference between the received signal and the noise floor to detect the presence of a received signal.

III. THE PROPOSED SYSTEM ARCHITECTURE

Figure 2 depicts an overview of the proposed system. The figure shows that the proposed system constitutes three stages: the phase detection stage, the preprocessing stage and the processing stage. The phase detection stage consists of three antenna elements, three two-ways RF splitters, and four phase detectors. The first three phase detectors, that are connected to the blue antennas, are used to estimate the phase difference between the antenna pairs. The gain difference of the fourth phase detector, that is connected to the red antenna from one side and to an open circuit from the other side, will be used as a trigger to start the recording process. The preprocessing stage consists of four analogue-to-digital (ADC) components that convert the analogue outputs of the phase detectors to digital values, and a LoRa module which is used to pack the digitized phase values in a LoRa packet. The LoRa packet, then, will be transmitted to the nearest LoRaWAN gateway.

The collection process of the phase values will start as the RF signal impinges on the antenna elements. Consequently, the gain detector will trigger the phase detectors to start the phase recording process. The recorded digital phase values will be packed and sent to the cloud. In the cloud, the processing stage will be performed (see Section IV). Accordingly, no heavy processing is conducted by the AoA estimation hardware, hence, the proposed system can be considered a low power AoA estimation system.

IV. THE PROPOSED AOA ESTIMATION ALGORITHM

Assume an RF signal impinges on an array antenna, then, the received signal vector can be expressed as

$$\mathbf{x}(t) = [x_1(t) \dots x_n(t) \dots x_N(t)]^T, \quad (1)$$

in which

$$x_n(t) = A_r e^{i2\pi f_c t} e^{i\psi_n(\theta)} + \omega_n, \quad (2)$$

where $(\cdot)^T$ is the transpose notation, A_r is the received signal's amplitude, f_c is the carrier frequency, and ω_n is the identically independently distributed (iid) complex-valued Gaussian noise with zero-mean and variance σ^2 ; i.e. $CN(0, \sigma^2)$. $\psi_n(\theta)$ is the phase difference between the n^{th} element in the array antenna and a reference point in space. $\psi_n(\theta)$ is a function of θ , where $\{\theta \in R : -\pi \leq \theta \leq \pi\}$ is the azimuth angle.

The proposed system, see figure 2, constitutes three antennas that are distributed over a triangle surface and

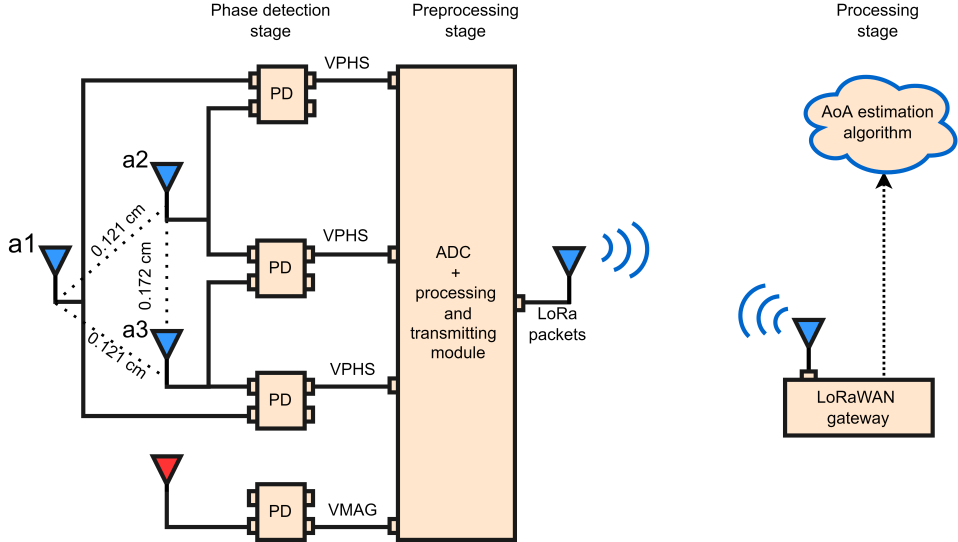


Fig. 2: A schematic representation of the proposed system, which constitutes three stages: the phase detection, the preprocessing and the processing stages. The phase detection stage consists of three antenna elements, three two-ways RF splitters, and four phase detectors. The first three phase detectors, that are connected to the blue antennas, are used to estimate the phase difference between the antenna pairs. The gain difference of the fourth phase detector, that is connected to the red antenna from one side and to an open circuit from the other side, will be used as a trigger to start the phase recording process. The preprocessing stage consists of four ADC components, and a LoRa module which is used to pack the digitized phase values in a LoRa packet. The LoRa packet, then, will be transmitted to the nearest LoRaWAN gateway. In the cloud, the AoA estimation process will be conducted.

the phase difference values between every pair can be expressed as follows

$$\begin{aligned}\psi_{12}(\theta_r) &= \psi_1 - \psi_2, \\ \psi_{13}(\theta_r) &= \psi_1 - \psi_3, \\ \psi_{23}(\theta_r) &= \psi_2 - \psi_3,\end{aligned}\quad (3)$$

where θ_r is the AoA of the received signal.

In this paper, we have utilized the multivariate normal probability density function to estimate the AoA of the received signals as follows

$$\begin{aligned}\mathbf{y}(\theta) &= \mathcal{N}(\Psi(\theta), \Psi_r, \Sigma) \\ &= \exp\left(-\frac{1}{2} (\Psi(\theta) - \Psi_r)^T \Sigma^{-1} (\Psi(\theta) - \Psi_r)\right),\end{aligned}\quad (4)$$

Σ is the distribution's covariance matrix and is given by

$$\Sigma = \sigma^2 I_3, \quad (5)$$

where σ^2 is the variance of the normal distribution and I_3 is the identity matrix of size (3×3) . Ψ_r is the received phase response vector, which contains three phase difference values that are associated with the AoA of the received signal, and can be expressed as follows

$$\Psi_r = [\psi_{12}(\theta_r) \ \psi_{13}(\theta_r) \ \psi_{23}(\theta_r)]^T. \quad (6)$$

$\Psi(\theta)$ is the phase response vector, which contains all the possible phase difference values for all the possible receiving angles, and can be expressed as follows

$$\Psi(\theta) = [\psi_{12}(\theta) \ \psi_{13}(\theta) \ \psi_{23}(\theta)]^T, \quad (7)$$

$$\begin{aligned}\psi_{12}(\theta) &= \frac{2\pi}{\lambda} d_{12} \sin\left(\theta - \frac{\pi}{4}\right), \\ \psi_{13}(\theta) &= \frac{2\pi}{\lambda} d_{13} \sin\left(\theta + \frac{\pi}{4}\right), \\ \psi_{23}(\theta) &= \frac{2\pi}{\lambda} d_{23} \sin(\theta),\end{aligned}\quad (8)$$

$d_{11} = 0.35\lambda$, $d_{13} = 0.35\lambda$ and $d_{23} = 0.5\lambda$ are the inter-element spacing between $a1$ and $a2$ antennas, $a1$ and $a3$ antennas, and $a2$ and $a3$ antennas, respectively. λ the received signal's wavelength. Finally, the AoA of the received signals can be estimated as follows

$$\text{AoA} = \underset{\theta}{\operatorname{argmax}}(\mathbf{y}(\theta)). \quad (9)$$

V. EXPERIMENTAL ANALYSES

To validate the proposed system, we have conducted an experiment in an anechoic chamber; see figure 3. The triangle antenna elements were placed over a pan-tilt system. Every antenna pair of the triangle side has been connected to a phase detector. The gain detector is placed near the preprocessing unit. The preprocessing unit starts packing the phase values as soon as the gain detector detects a signal. Afterwards, the preprocessing unit transmits the packed phase values to the nearest LoRaWAN gateway.

A LoRa transmitter (transmits LoRa signals of 125 kHz

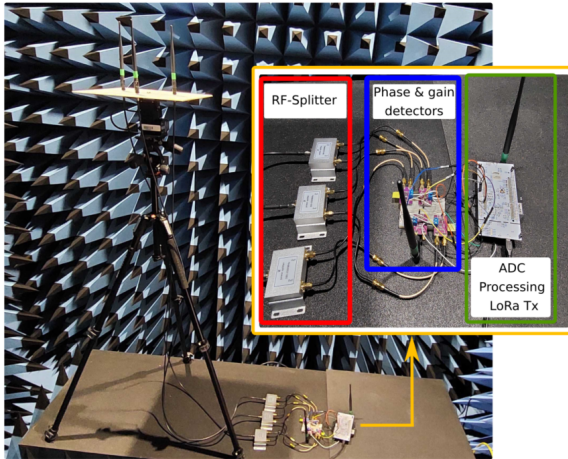


Fig. 3: The experimental setup. Three dipole elements were distributed over a triangle surface (with inter-element spacing as shown in figure 2). The antenna elements were installed on the top of a pan-tilt system. A LoRa transmitter was placed 3 meters away from the antennas to act as a target.

bandwidth with spreading factor of 12 at 868 MHz frequency band) was placed in front of the pan-tilt system. During the experiment, we were rotating the triangle antenna elements from -85° to 85° in steps of 5° . For every azimuth angle, 10 phase values were recorded from each phase detector; yielding 350 phase values were considered throughout the entire experiment.

Figures 4 a) and b) show respectively the estimation vectors $\mathbf{y}(\theta)$, see Eq.4, of a single antenna pair (a2 and a3 antennas, see figure 2) and the triangle antenna elements pairs. The target was placed at azimuth angle 30° . It is obvious, unlike the proposed triangle antennas structure, the estimation vector $\mathbf{y}(\theta)$ of the single antenna pair has two maximum regions. Accordingly, there will be an AoA estimation ambiguity between angles 30° and -30° . Figures 4 c) and d) show the pairwise Euclidean distance of the search space, i.e. the Euclidean distance of the estimation vectors $\mathbf{y}(\theta)$ considering all the possible values of θ . The estimation vectors $\mathbf{y}(\theta)$ of a single antenna pair (a2 and a3 antennas, see figure 2) and the triangle antenna elements pairs were respectively considered in figure c) and d). Off diagonal areas with small Euclidean distances (i.e. large ambiguities) can be observed significantly in figure c). Consequently, a single antenna pair will always provide an ambiguity between the positive and negative angles. On the other hand, the proposed triangle antenna structure provides clear small Euclidean distances for the diagonal area. Therefore, a unique AoA estimation can be expected for the proposed antenna structure.

Figure 5 shows the Cumulative Distribution Function (CDF) for the AoA estimation error of all the received signals. The median and maximum estimation errors equal 4 and 14 degrees, respectively. The inner figure shows the

AoA estimate for every azimuth angle. The red circles represent the AoA estimates and the blue line represents the exact angle between the transmitter and the proposed system. One can deduce that the AoA estimates are very close to the exact angles. Furthermore, the proposed hardware architecture and the AoA estimation algorithm can provide accurate estimation for both the broadside and endfire regions of the triangle antennas structure.

VI. CONCLUSION

In this paper, we have proposed a comprehensive low-power and low-cost Angle of Arrival (AoA) estimation system. The proposed system consists of a hardware architecture and an AoA estimation algorithm. The proposed hardware architecture is generic (it can cover signals up to 2.7GHz frequency and 30 MHz bandwidth), low cost (it consists of low cost commercial off-the-shelf components), and consumes low power (it operates with minimal computational complexity). Accordingly, the proposed system can provide AoA estimates in areas with poor infrastructure or it can be used as a mobile AoA estimation unit. The experimental validation, which has been conducted in a controlled environment, reveals that the proposed hardware can estimate the AoA of the received signals from various azimuth angles with median and maximum estimation errors of 4 and 14 degrees, respectively. Although the proposed system had provided a good performance in an anechoic chamber, the system performance should be tested in a realistic environment where the multipath effect is inevitable.

REFERENCES

- [1] M. Aernouts, N. BniLam, R. Berkvens, and M. Weyn, "TDAoA: A combination of TDoA and AoA localization with LoRaWAN," *Internet of Things*, vol. 11, p. 100236, 2020.
- [2] M. Aernouts, B. Bellekens, R. Berkvens, and M. Weyn, "A comparison of signal strength localization methods with Sigfox," in *2018 15th Workshop on Positioning, Navigation and Communications (WPNC)*. IEEE, 2018, pp. 1–6.
- [3] T. Janssen, M. Weyn, and R. Berkvens, "A primer on real-world RSS-based outdoor NB-IoT localization," in *2020 International Conference on Localization and GNSS (ICL-GNSS)*. IEEE, 2020, pp. 1–6.
- [4] N. BniLam, G. Ergeerts, D. Subotic, J. Steckel, and M. Weyn, "Adaptive probabilistic model using angle of arrival estimation for iot indoor localization," in *2017 International Conference on Indoor Positioning and Indoor Navigation (IPIN)*. IEEE, 2017, pp. 1–7.
- [5] N. Bnlam, E. Tanghe, J. Steckel, W. Joseph, and M. Weyn, "ANGLE: ANGular Location Estimation algorithms," *IEEE Access*, vol. 8, pp. 14 620–14 629, 2020.
- [6] N. Bnlam, D. Joosens, R. Berkvens, J. Steckel, and M. Weyn, "AoA-based localization system using a single IoT gateway: An application for smart pedestrian crossing," *IEEE Access*, vol. 9, pp. 13 532–13 541, 2021.
- [7] J. Steckel, D. Laurijssen, A. Schenck, N. BniLam, and M. Weyn, "Low-cost hardware platform for angle of arrival estimation using compressive sensing," in *12th European Conference on Antennas and Propagation (EuCAP 2018)*. IET, 2018, pp. 1–4.
- [8] N. Bnlam, J. Steckel, and M. Weyn, "Synchronization of multiple independent sub-array antennas for IoT applications," in *12th European Conference on Antennas and Propagation (EuCAP 2018)*. IET, 2018, pp. 1–5.

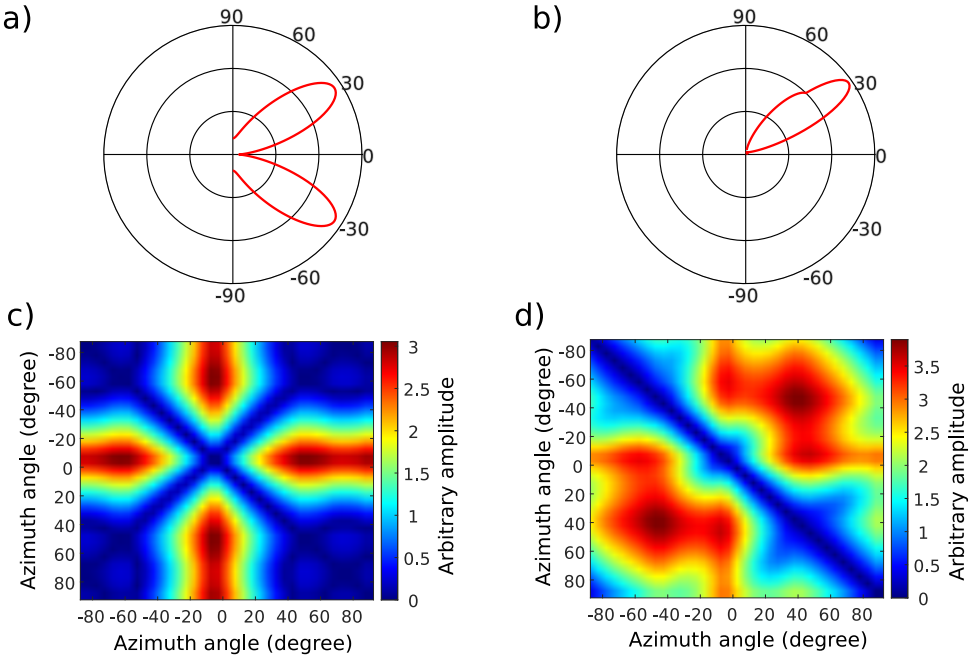


Fig. 4: Figures a) and b) show respectively the estimation vectors $y(\theta)$, see Eq.4, of a single antenna pair (a2 and a3 antennas, see figure 2) and the triangle antenna elements pairs. The target was placed at azimuth angle 30° . Figures c) and d) show the pairwise Euclidean distance of the search space, i.e. the Euclidean distance between the estimation vectors $y(\theta)$ considering all the possible values of θ . The estimation vectors $y(\theta)$ of a single antenna pair (a2 and a3 antennas see figure 2) and the triangle antenna elements pairs were respectively considered in figure c) and d). The arbitrary amplitudes in the pairwise figures can be used as an indicator for the uniqueness of the estimator, e.g. a perfect estimator should only provide zero arbitrary amplitudes along the diagonal area of the figure.

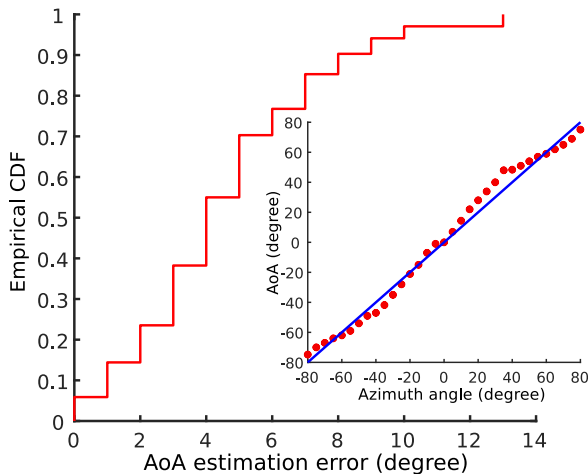


Fig. 5: The CDF for the AoA estimation error of all the received signals. The median and maximum estimation errors of 4 and 14 degrees, respectively. The inner figure shows the AoA estimate for every azimuth angle. The red circles represent the AoA estimates and the blue line represents the exact angle between the transmitter and the proposed system.

- [9] N. BniLam, J. Steckel, and M. Weyn, "Synchronization of Multiple Independent Subarray Antennas: An Application for Angle of Arrival Estimation," *IEEE Transactions on Antennas and Propagation*, vol. 67, no. 2, pp. 1223–1232, 2019.

- [10] N. BniLam, D. Joosens, J. Steckel, and M. Weyn, "Low cost AoA unit for IoT applications," in *2019 13th European Conference on Antennas and Propagation (EuCAP)*. IEEE, 2019, pp. 1–5.
- [11] N. BniLam, D. Joosens, M. Aernouts, J. Steckel, and M. Weyn, "LoRay: AoA estimation system for long range communication networks," *IEEE Transactions on Wireless Communications*, vol. 20, no. 3, pp. 2005–2018, 2020.
- [12] K.-J. Baik, S. Lee, and B.-J. Jang, "Hybrid RSSI-AoA positioning system with single time-modulated array receiver for LoRa IoT," in *2018 48th European Microwave Conference (EuMC)*. IEEE, 2018, pp. 1133–1136.
- [13] G. Avitabile, A. Florio, and G. Covillello, "Angle of arrival estimation through a full-hardware approach for adaptive beamforming," *IEEE Transactions on Circuits and Systems II: Express Briefs*, 2020.
- [14] P.-C. Chiang, W.-J. Liao, Y.-T. Tu, and H.-C. Liu, "Implementation of direction-of-arrival estimation using rotman lens array antenna," in *2013 International Symposium on Electromagnetic Theory*. IEEE, 2013, pp. 855–858.
- [15] N. BniLam, A. Aerts, D. Joosens, J. Steckel, and M. Weyn, "RSS-based AoA estimation system for IoT applications using Rotman lens," in *2020 14th European Conference on Antennas and Propagation (EuCAP)*. IEEE, 2020, pp. 1–5.
- [16] A. Devices, "Ad8302, lf-2.7 ghz rf/if gain and phase detector," *Preliminary Data Sheet*, 2002.
- [17] P. R. Maus, "Phase and Amplitude Stability of a Pulsed RF System on the Example of the CLIC Drive Beam LINAC," Nov 2016, presented 01 Mar 2017. [Online]. Available: <https://cds.cern.ch/record/2274101>
- [18] J. P. Balsamo, "Phase and Amplitude Interferometry Based Radio Frequency Direction Finder," 2019. [Online]. Available: <https://scholars.unh.edu/honors/450/>